Electronic Supplementary Information (ESI)

Light and cucurbit[7]uril complexation dual-responsiveness of a cyanostilbene–based self-assembled system

Pengyao Xing,[a] Hongzhong Chen,[b] Mingfang Ma,[a] Xingdong Xu,[b] Aiyou Hao* [a] and Yanli Zhao[b, c]

[a] Key Laboratory of Colloid and Interface Chemistry of Ministry of Education and School of Chemistry and Chemical Engineering, Shandong University, Jinan 250100, PR China

[b] Division of Chemistry and Biological Chemistry, School of Physical and Mathematical Sciences, Nanyang Technological University, 21 Nanyang Link, Singapore 637371, Singapore. E-mail: zhaoyanli@ntu.edu.sg

[c]School of Materials Science and Engineering, Nanyang Technological University, Singapore 639798, Singapore

1. Experimental section

Materials

All chemicals were purchased from Sigma-Aldrich and used without further purification. Before use, acetone was re-distilled under reflux with potassium carboxylate. (Z)-2-(4-(10-Bromodecyloxy)phenyl)-3-(4-(dimethylamino)phenyl)acrylonitrile (compound 1) was synthesized according to our previous report[S1].

Characterizations

^{1}H NMR spectra were measured on a Bruker-AC 300 spectrometer. ^{13}C NMR spectrum was measured on a Bruker BBFO-400 spectrometer. The electronic spray ionization (ESI) mass spectra were recorded on a ThermoFinnigan LCQ quadrupole ion trap mass spectrometer. High-resolution mass spectrometry (HR-MS) was performed on a Waters Q-tof Premier MS spectrometer. Absorption spectra were recorded on a Shimadzu UV-3600 spectrophotometer. The fluorescence emission spectra were recorded on a Shimadzu RF-5301pc fluorescence spectrophotometer. The photoirradiation was carried on an ENF-260C/FBE UV lamp (4 W) with the irradiation wavelength of 254 nm in a 2 mm quartz cell. TEM images were collected on a JEM-1400 (JEOL). SEM images were collected from a SEM of field-emission JSM-6700F (JEOL). AFM images were recorded under ambient conditions by using a Veeco Nanoscope Multimode III SPM operating intapping mode. DLS size distributions were measured on a Nanobrook 90Plus particle size

analyzer.

Synthesis of CS

A solution of compound 1 (0.48 g, 1 mmol) and excess pyridine (0.79 g, 10 mmol) in acetonitrile (20 mL) stirred at 80 ^{o}C for 10 h. The reaction was monitored by TLC experiments. After all the compound 1 disappeared, the solvent was removed under reduced pressure. The residue was dispersed in distilled water, followed by the filtration under reduced pressure. The aqueous solution was freeze-dried to obtain the pure yellow compound CS (500 mg, 89 %). ^{1}H NMR (300 MHz, D_6 DMSO, 298 K). δ = 9.16 (d, 2H), 8.60 (t, 1H), 8.14 (t, 2H), 7.85 (t, 2H), 7.68 (s, 1H), 7.61 (d, 2H), 7.01 (d, 2H), 6.82 (d, 2H), 4.60 (t, 2H), 4.02 (t, 2H), 3.02 (s, 6H), 1.91 (t, 2H), 1.74 (t, 2H), 1.20-1.49 (m, 12H). ^{13}C NMR (100 MHz, $CDCl_3$, 298 K) δ = 159.88, 151.48, 145.78, 145.12, 144.49, 131.83, 130.95, 130.14, 128.43, 126.77, 125.13, 121.89, 120.84, 115.54, 111.95, 111.77, 106.07, 68.02, 60.84, 31.27, 29.56, 28.73, 25.78. HRMS (TOF) m/z $[M+H]^+$, calcd for $C_{32}H_{40}N_3O$, 482.3171; found, 482.3165.

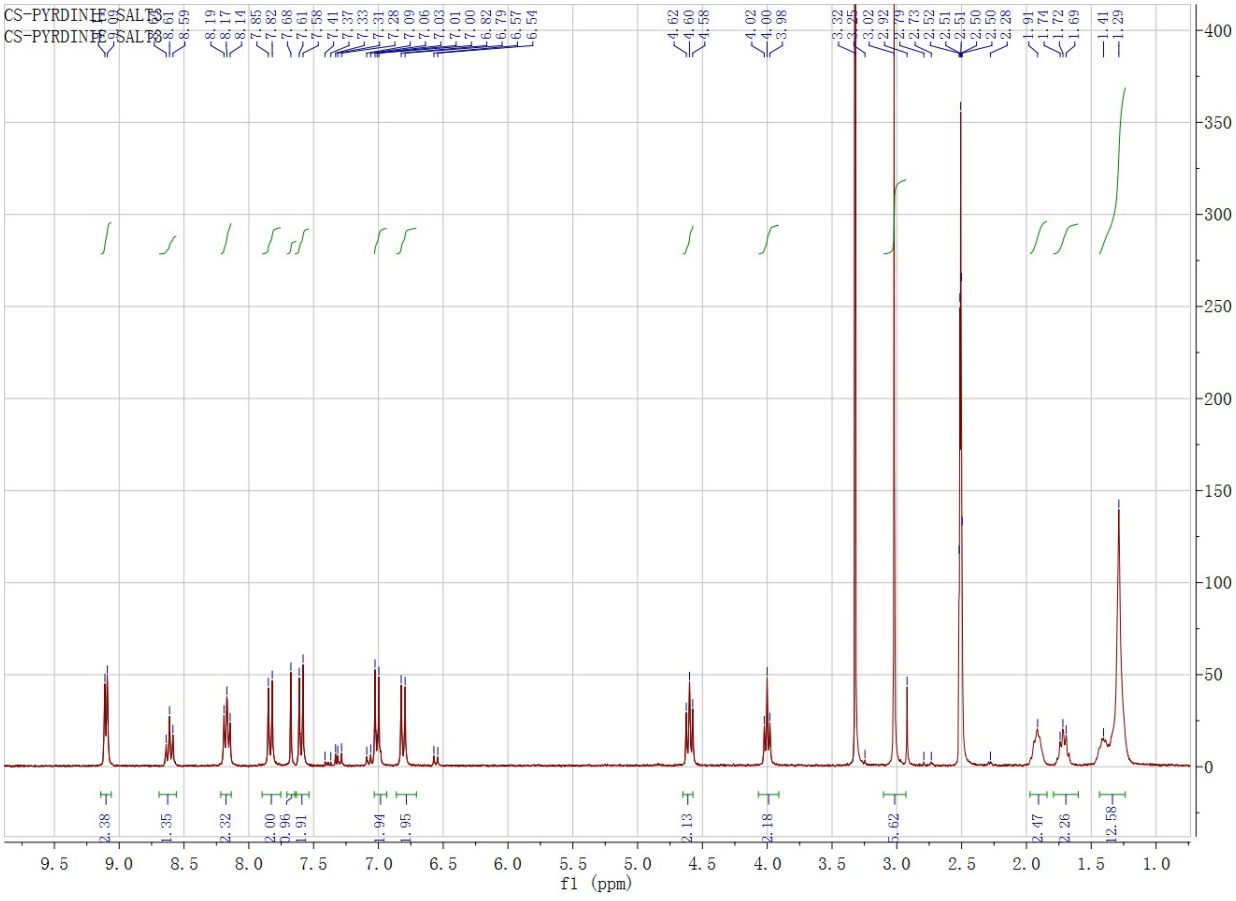

^{1}H NMR spectra of CS in D_6 DMSO.

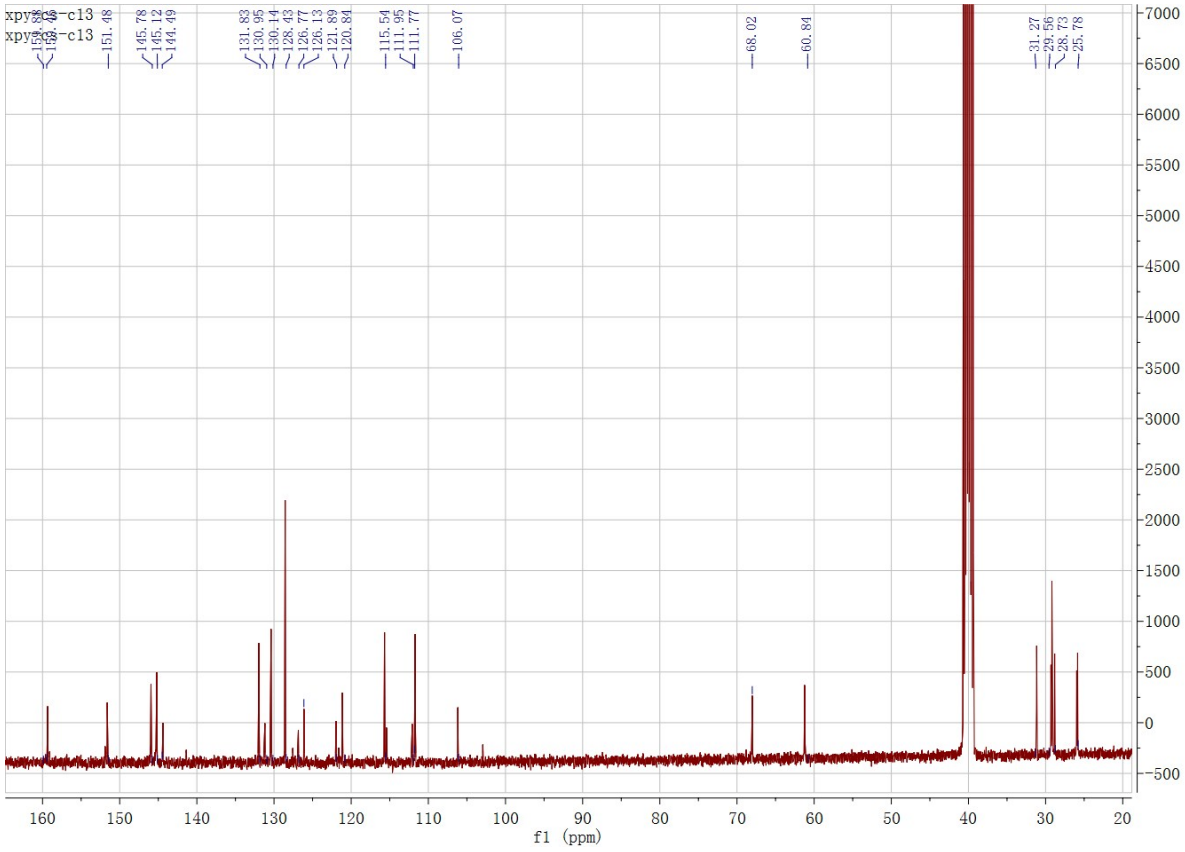

^{13}C NMR spectra of CS in D_6 DMSO.

2. Self-assembly behaviors of CS

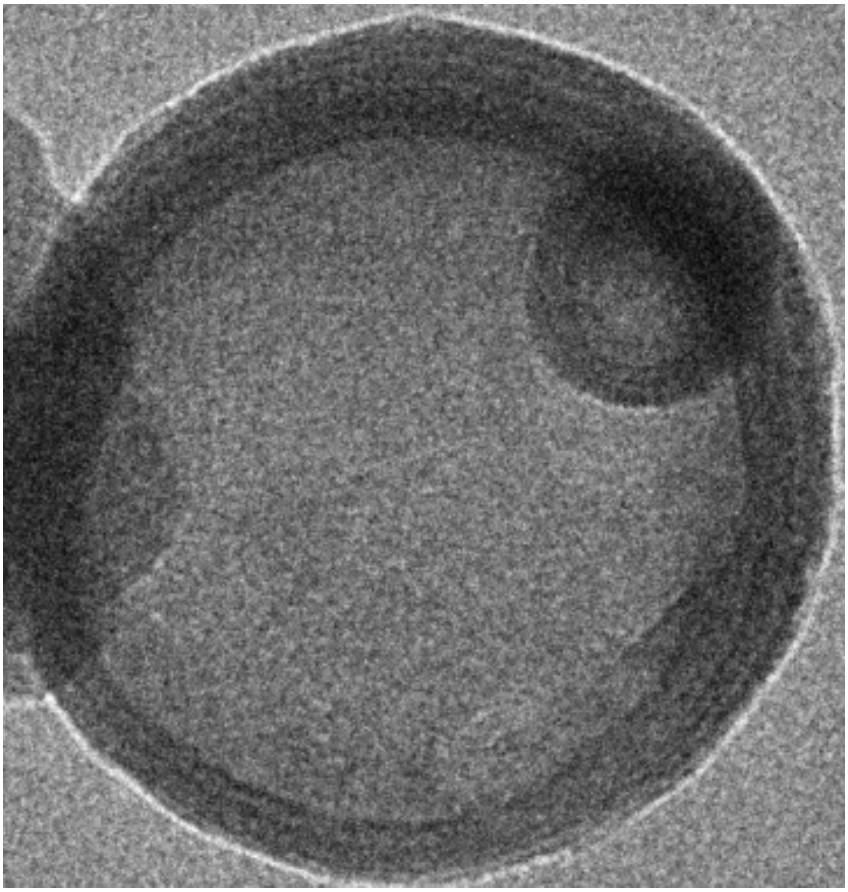

Figure S1. The enlarged TEM image of the inset of Fig. 1a, of which vesicle wall consists of up to five layers, indicating its multi-lamellar nature.

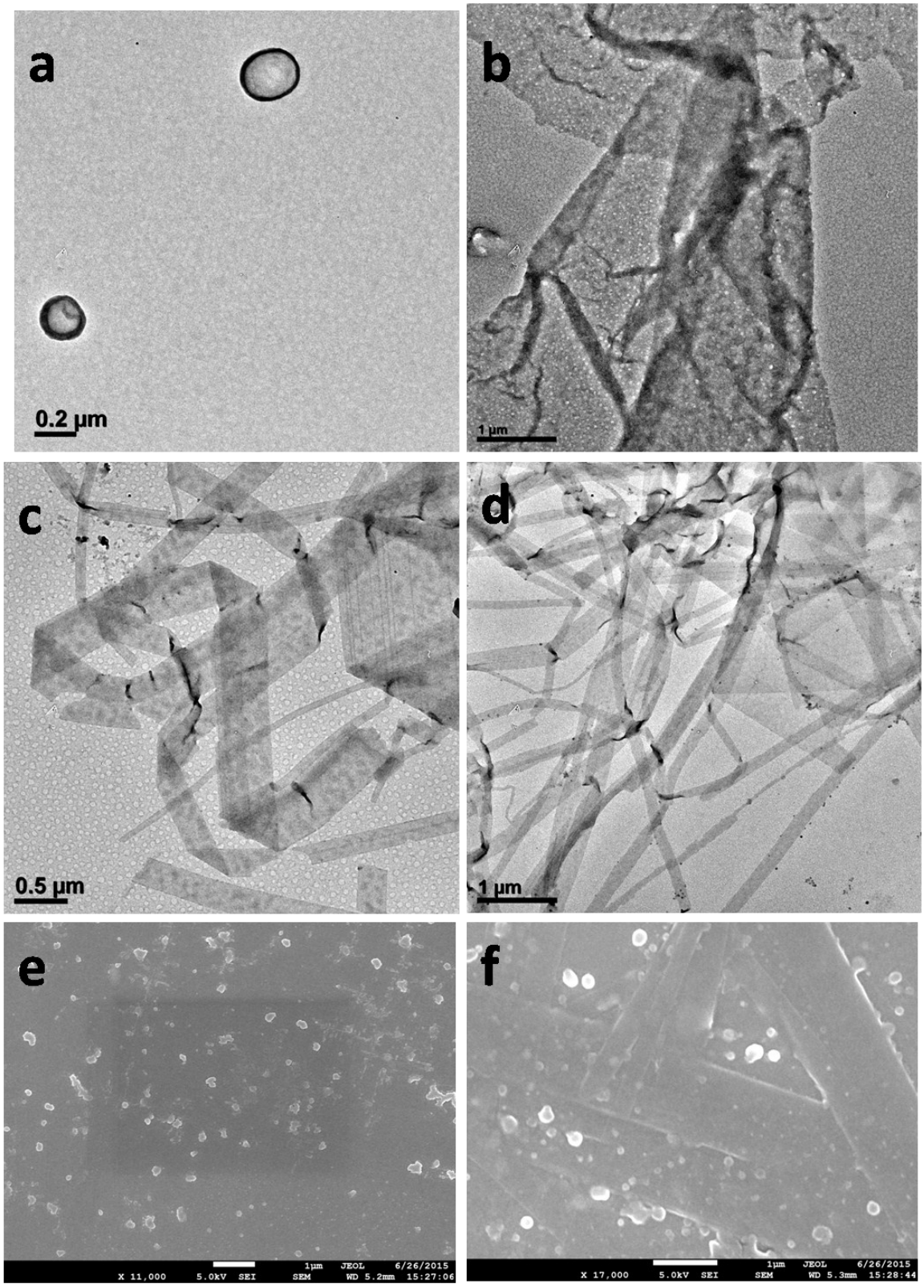

Figure S2 (a-b) TEM images of vesicles and nanoribbons found in CS system ($5x10^{-4}$ M). (c-d) TEM images of the nanoribbons found in CS system (10^{-3} M). (e-f) SEM images of vesicles (10^{-4} M) and co-existance of vesicles/nanoribbons (10^{-3} M).

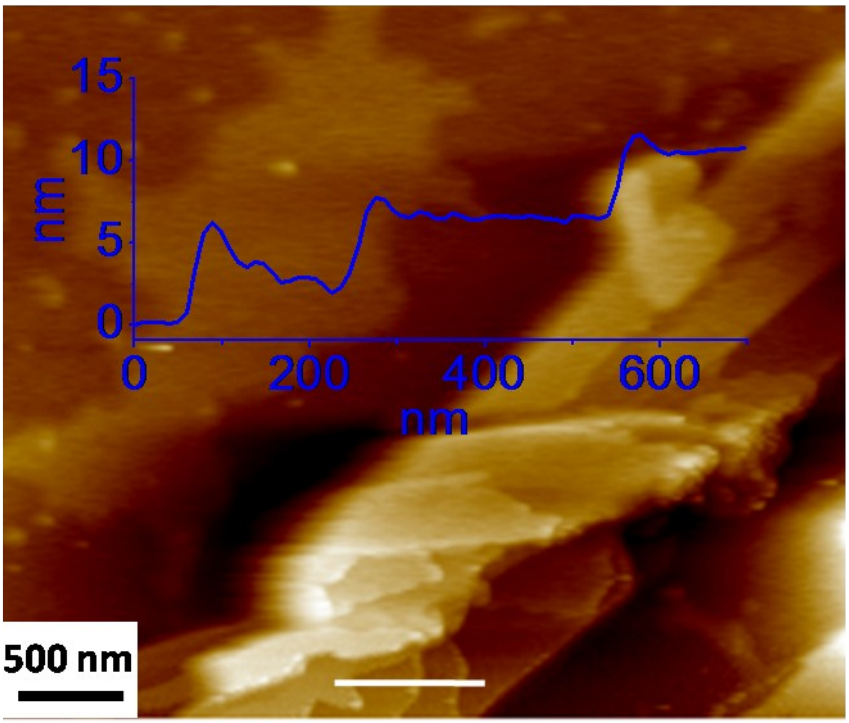

Figure S3 AFM image and height profile of the nanoribbons. A value of ca. 5 nm was obtained, which suggested the bilayer length of CS molecules.

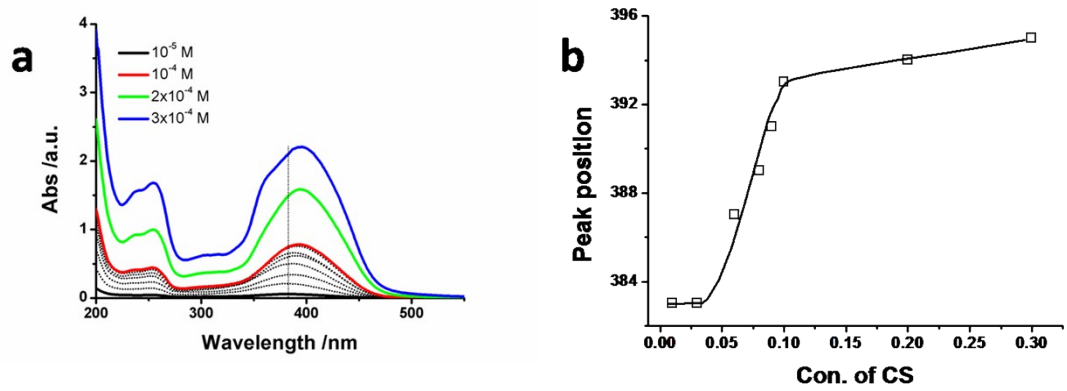

Figure S4 (a) Concentration-dependent UV-vis spectra of CS in aqueous media. (b) Peak position locations with the increaseing of CS concentration (mM). From (b), the critical aggregation concentration of CS in aqueous media can be determined as 0.06 mM.

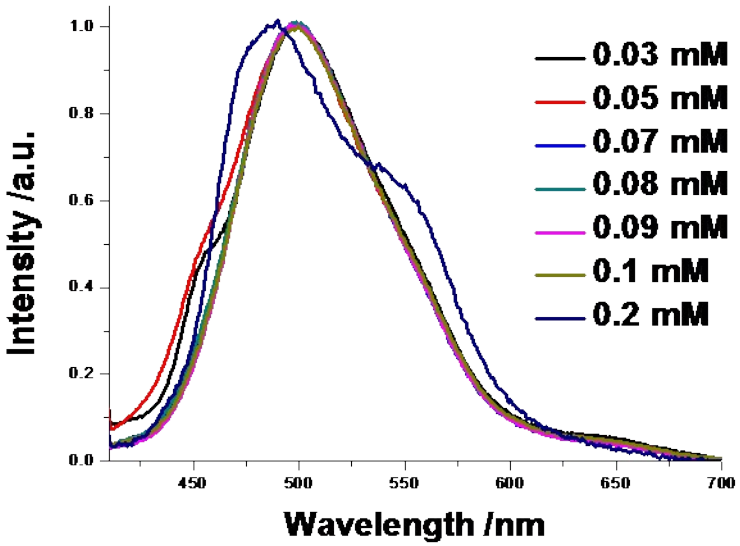

Figure S5 Normalized emission spectra of CS with different concentrations in water.

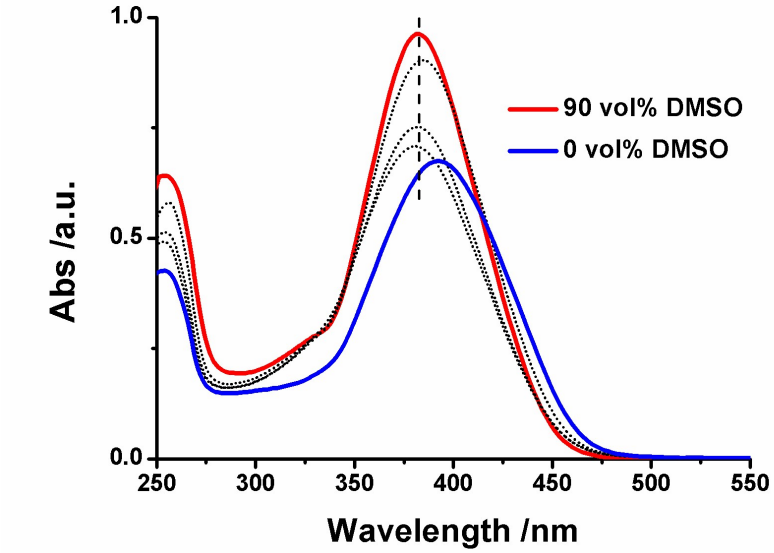

Figure S6 UV-vis spectra of the CS system with different DMSO volume fractions from 90 vol% to 0 vol%. The concentration of CS was fixed at 10^{-4} M.

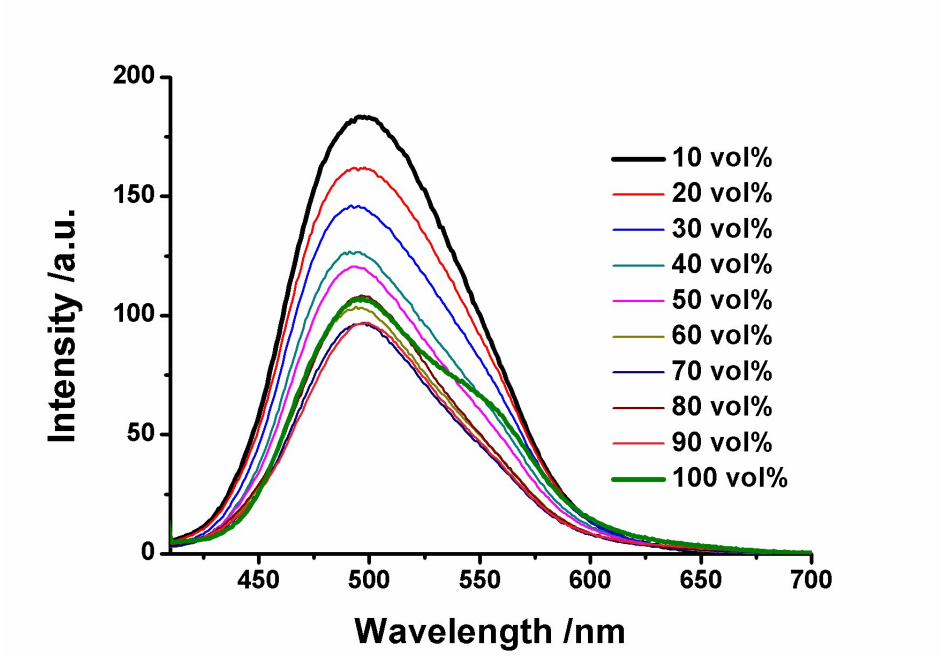

Figure S7 Emission spectra of the CS system with different water volume fractions from 10 vol% to 100 vol%. The concentration of CS was fixed at 10^{-4} M.

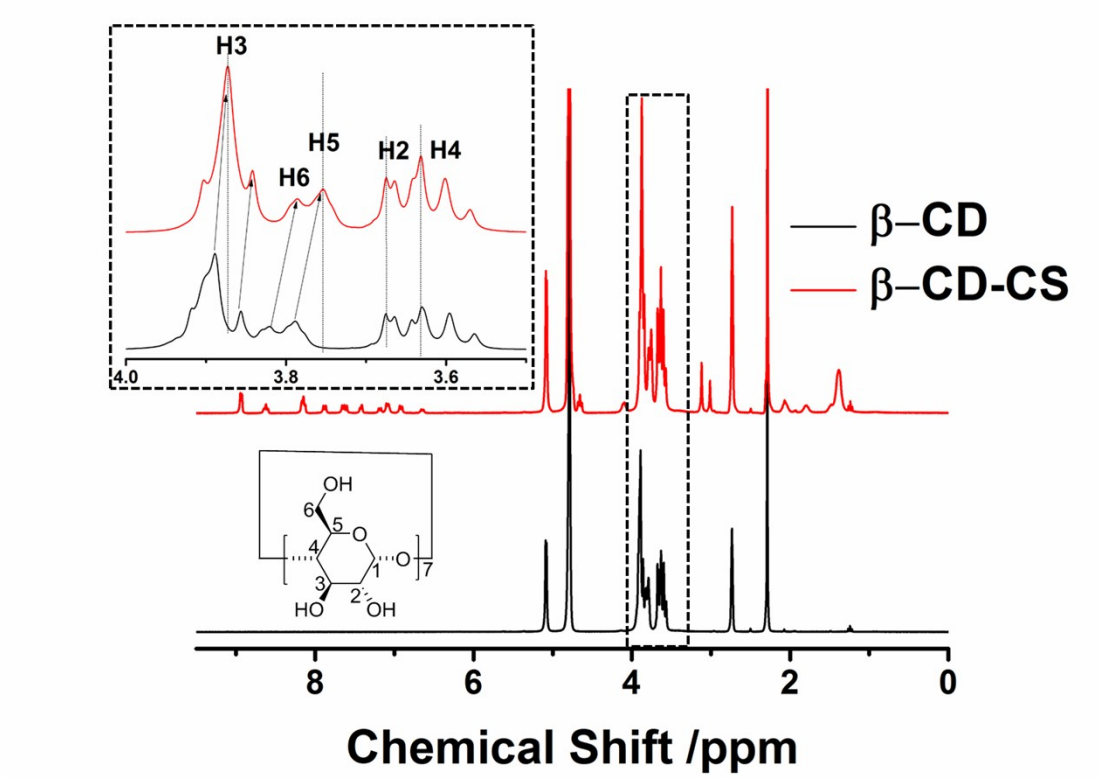

Figure S8 ^{1}H NMR comparison of β-cyclodextrin and β-cyclodextrin-CS complex in D_2O/D_6 DMSO mixture (6/4, v/v).

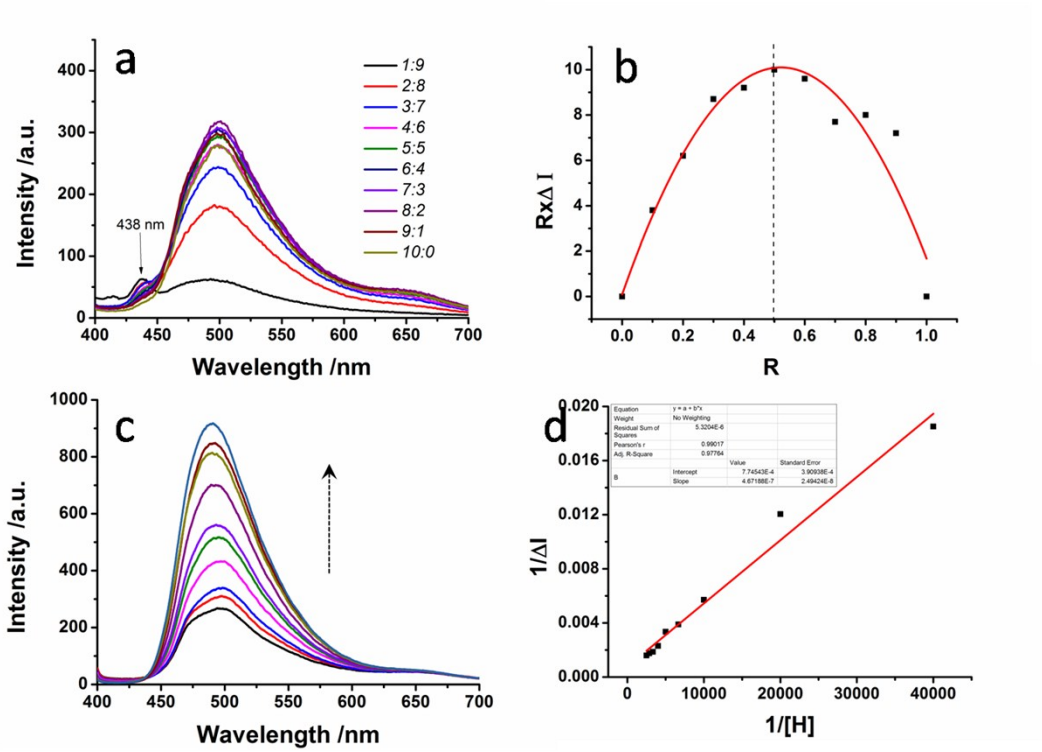

Figure S9 (a) Emission spectra of β-cyclodextrin-CS complex with different molar ratio (the total concentration was fixed at 10^{-4} M). (b) Job's plot calculated from (a), which indicates a 1:1 binding ratio. (c) Emission spectra of CS (10^{-4} M) with the addition of β- cyclodextrin from 0 molar equiv. to 4 molar equiv.. (d) Determination of equilibrium constant (k) via fluorescent titration according to Benesi–Hildebrand equation. A binding constant value of 1648 M^{-1} was obtained from (d).

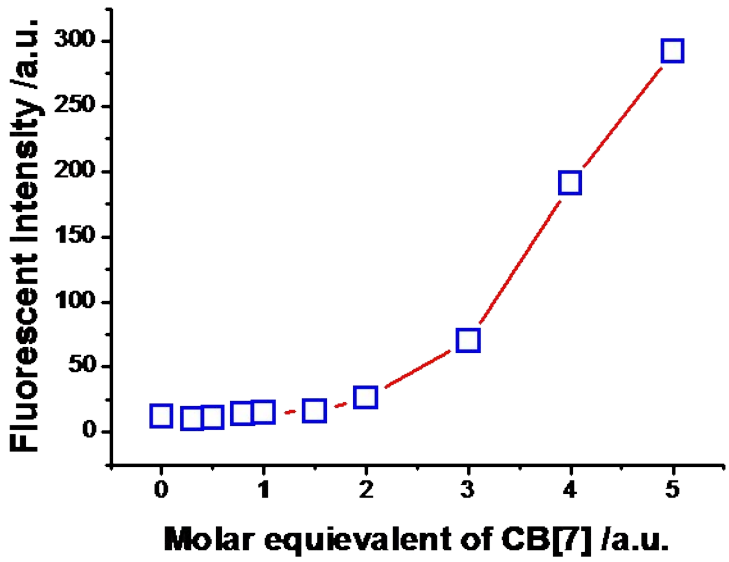

Figure S10 Fluorescent intensity as a function of molar ratio of CB[7] to CS. Concentration of CS was

fixed at 10^{-4} M.

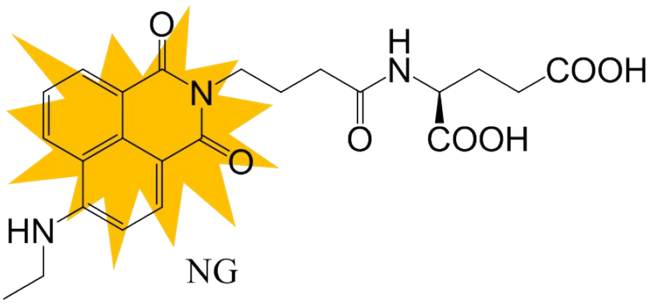

Scheme S1 Chemical structure of NG with yellow-orange luminescent color in water.

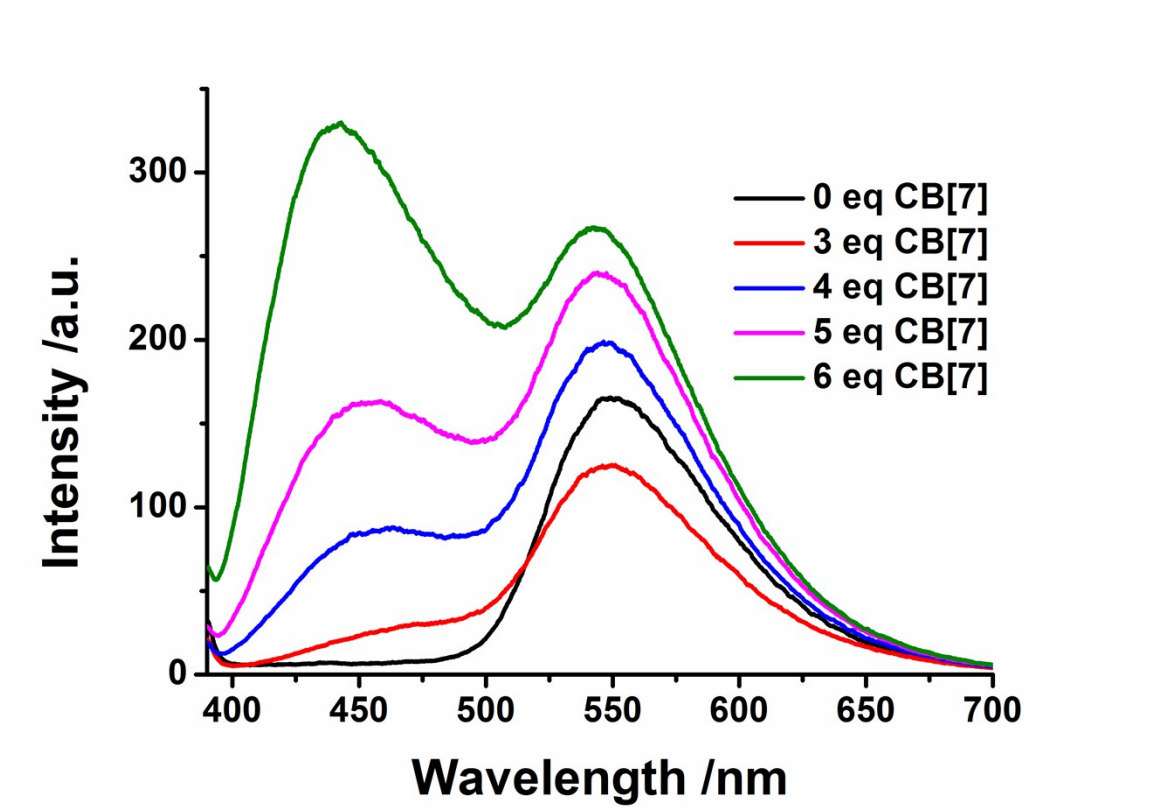

Figure S11 Emission spectra of CS-NG hybrids (both concentrations were controlled to 10^{-4} M) excited at 380 nm with the increase in CB[7] concentration in aqueous media.

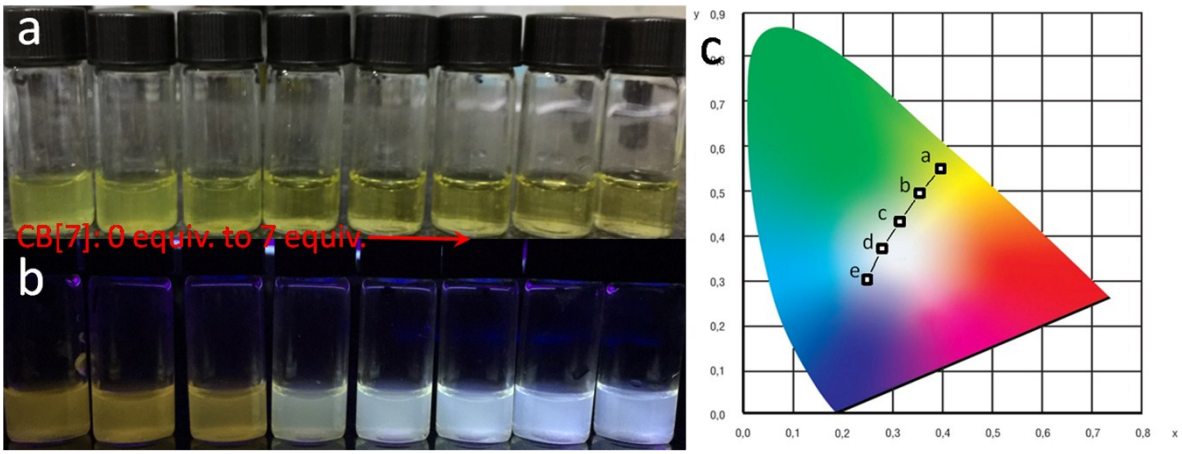

Figure S12 Digital images of CS-NG system with the increase in the molar equivalent of CB[7] from 0 equiv. to 7 equiv. under natural (a) and UV light (b, 365 nm). (c) CIE 1931 chromaticity diagram displaying the luminescent color coordinates. (a) to (e) stand for the molar equivalent of 0, 4, 5, 6, 7 respectively. CIE coordinates of (a) to (e) respectively: (0.40, 0.55), (0.36, 0.49), (0.32, 0.43), (0.28, 0.37), (0.25, 0.30).

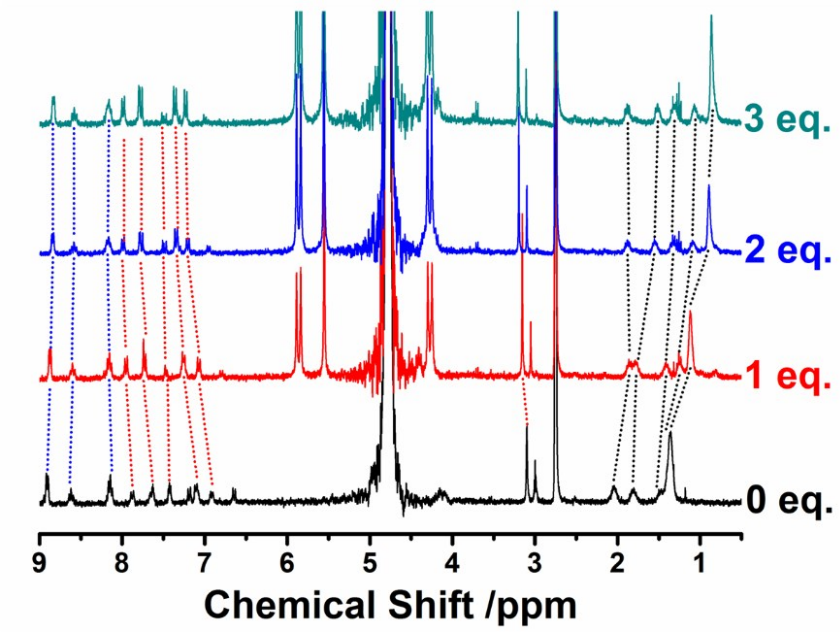

Figure S13 ^{1}H NMR full spectra of CS with different equivalent of CB[7].

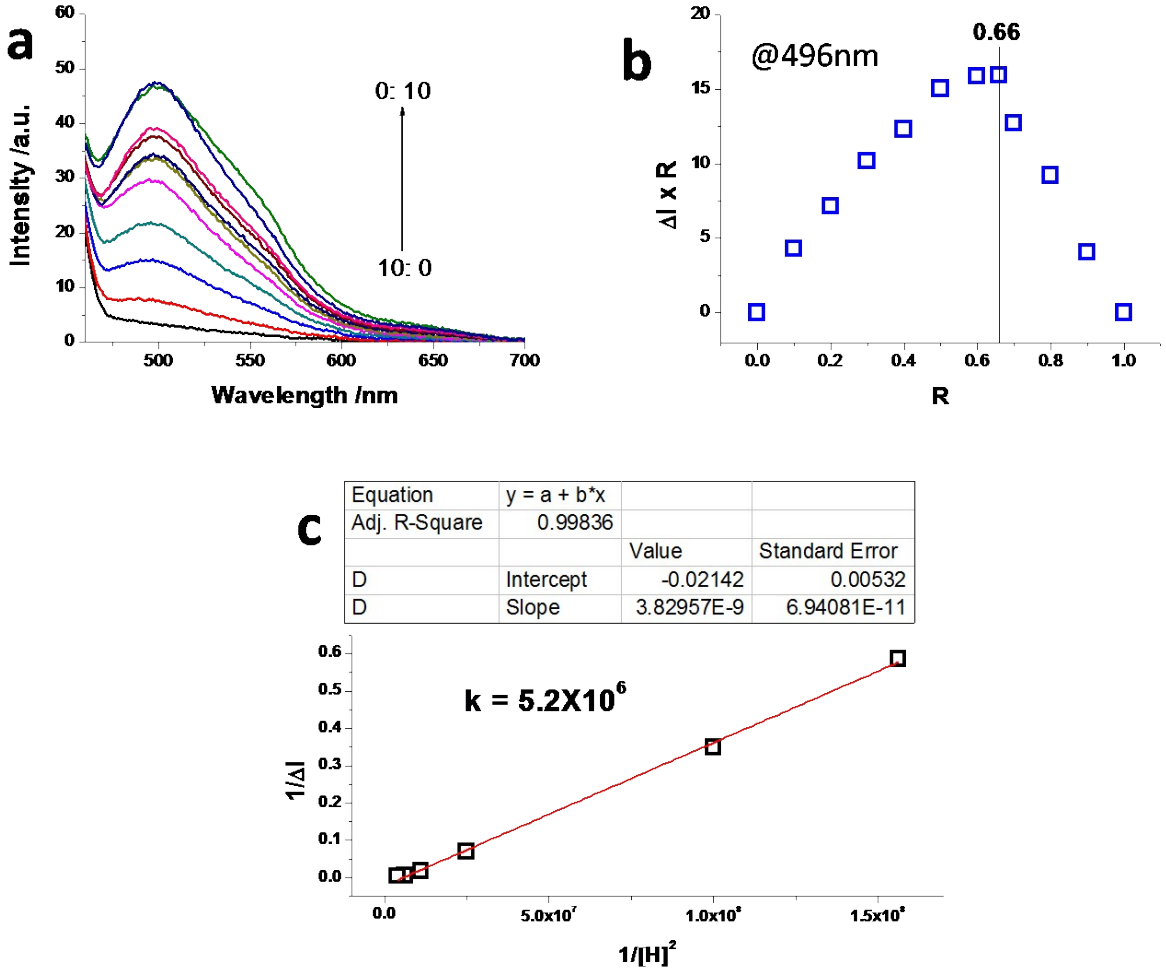

Figure S14. Determination of binding ratio by Job's plot (a-b) as well as the calculation of equilibrium constant (k) via fluorescent titration according to Benesi–Hildebrand equation.

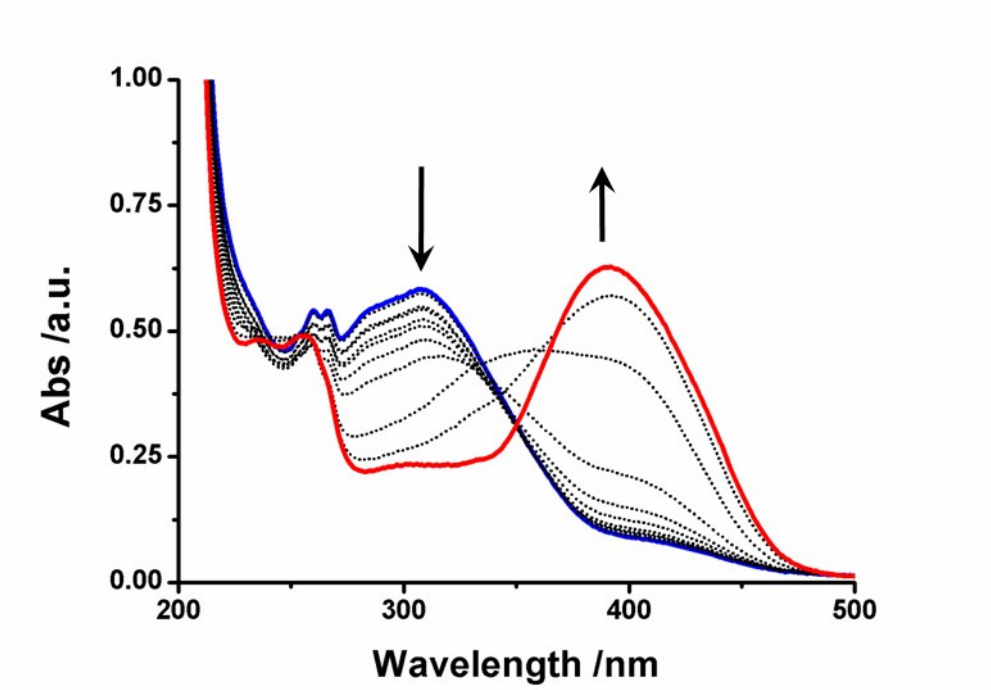

Figure S15 Changes of UV-vis spectra upon the addition of a competitive guest ADA into the CB[7]/CS complex solution (0-18 equiv.).

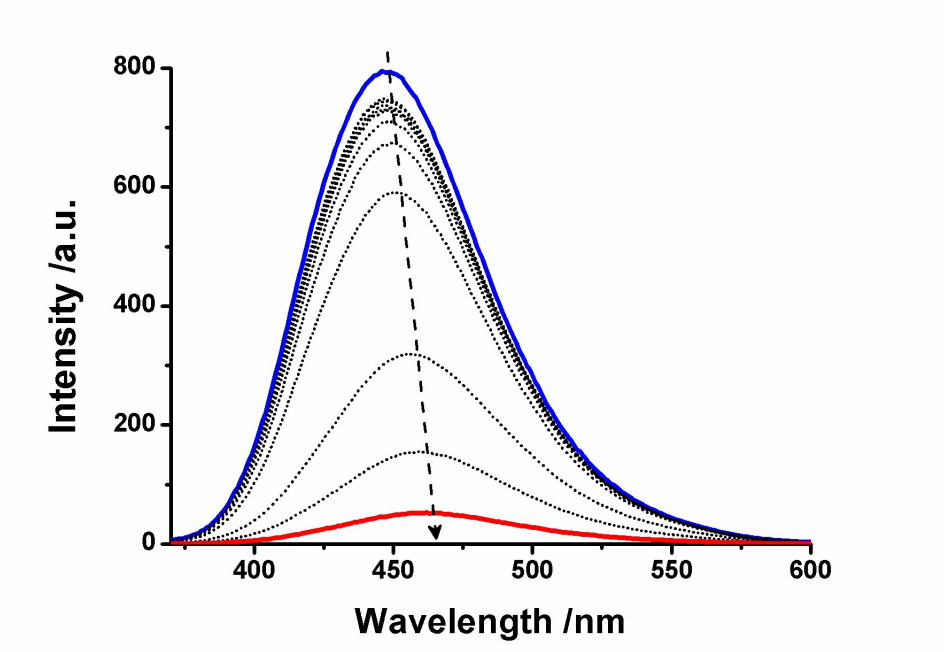

Figure S16 Changes of emission spectra upon the addition of a competitive guest ADA into the CB[7]/CS complex solution (0-18 equiv.).

3. Photo-responsiveness of CS and CB[7]/CS systems

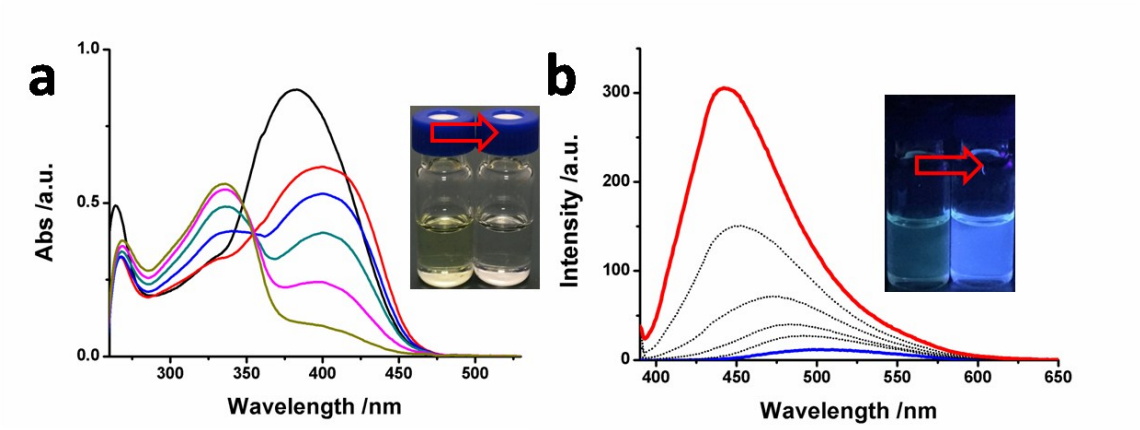

Figure S17 UV-vis (a) and emission spectra of CS solution in DMSO upon UV light irradiation with the same time intervals. Inset of (a) indicate the bulky color change from yellow to colorless. Inset of (b) stands for emission color change from weak yellow to bright blue under 365 nm light.

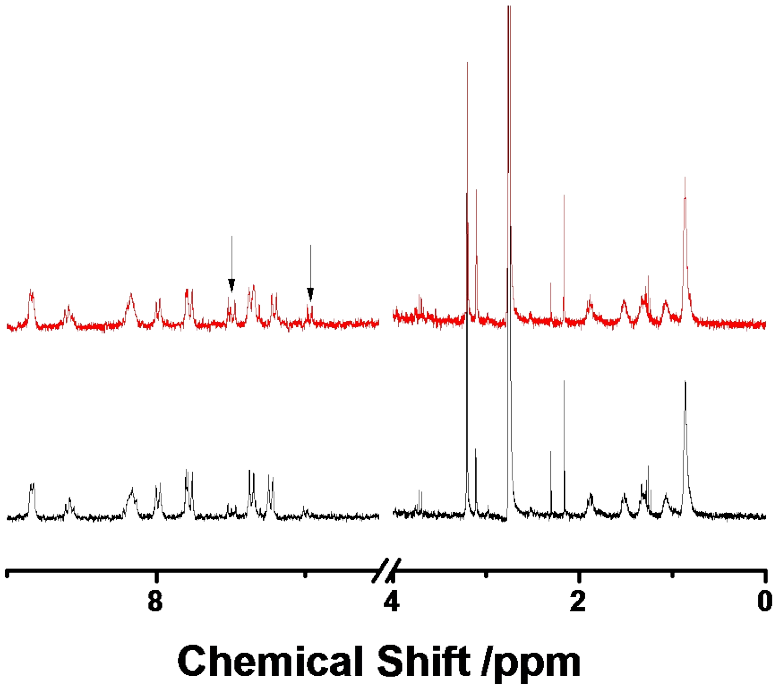

Figure S18 ^{1}H NMR change after UV light irradiation of CB[7]/CS system. The black arrows represent the existance of cis-isomers of CS after UV light treatment.

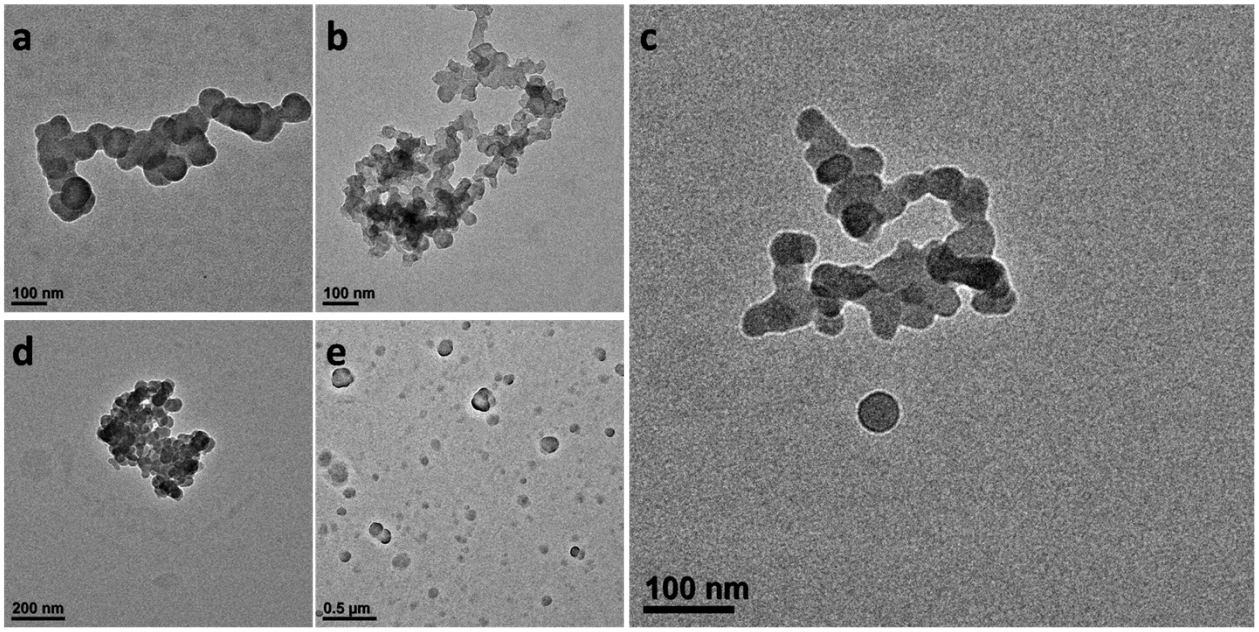

Figure S19 TEM images of small vesicles obtained from UV light treated vesicle samples (a-d, 10^{-4} M). We still found the presence of some initial vesicles due to the incomplete transformation (e).

4. References

S1. L. Zhu, C. Y. Ang, X. Li, K. T. Nguyen, S. Y. Tan, H. Ågren and Y. Zhao, *Adv. Mater*., 2012, **24**, 4020–4024.